Triazine containing N-rich microporous organic polymers for CO_2 capture and unprecedented CO_2/N_2 selectivity†

Subhajit Bhunia[a], Piyali Bhanja[a], Sabuj Kanti Das,[a] Tapas Sen,[b] and Asim Bhaumik[a*]

[a]*Department of Material Science, Indian Association for the Cultivation of Science, Jadavpur, Kolkata - 700032, India*

[a]*Nanobiomaterials Research Group, Centre for Materials Science, School of Physical Sciences and Computing, University of Central Lancashire, Preston, PR1 2HE, UK*

*Address for correspondence. Email: msab@iacs.res.in

†Electronic supplimentary information (ESI) available: BET specific surface area plot, thermal stability of SB-TRZ-CRZ and SB-TRZ-TPA, synthetic procedures, ^{13}C and ^{1}H NMR spectra.

Abstract

Targeted synthesis of microporous adsorbents for CO_2 capture and storage is very challenging in the context of remediation from green house gases. Herein we report two novel N-rich microporous networks SB-TRZ-CRZ and SB-TRZ-TPA by extensive incorporation of triazine containing tripodal moiety in the porous polymer framework. These materials showed excellent CO_2 storage capacities: SB-TRZ-CRZ displayed the CO_2 uptake capacity of 25.5 wt% upto 1 bar at 273 K and SB-TRZ-TPA gave that of 16 wt% under identical conditions. The substantial dipole quadruple interaction between network (polar triazine) and CO_2 boosts the selectivity for CO_2/N_2. SB-TRZ-CRZ has this CO_2/N_2 selectivity ratio of 377, whereas for SB-TRZ-TPA it was 97. Compared to other porous polymers, these materials are very cost effective, scalable and very promising material for clean energy application and environmental issues.

Keywords: CO_2 capture; CO_2/N_2 selectivity; porous organic polymers; N-rich frameworks.

1. Introduction

Climate change is a burning issue for our ecosystem and human beings due to tremendous emission of flue gas as a consequence of the industrial revolution [1]. The concentration of greenhouse gases (GHGs) such as CO_2, CH_4, NO_x are ascending day by day, which is primarily responsible for global warming [2]. Flue gas from coal powder holds roughly 12 to 15 wt% CO_2 at 40 ^{0}C temperature. Carbon di oxide is the predominant component of flue gas, which absorbs considerable amount of the solar heat energy and thus creates a barrier for the heat energy to leave the atmosphere [3]. Hence CO_2 concentration is a potent menacing factor for the future of the earth. In this context carbon capture and storage (CCS) is an excellent technology to capture, compression and permanent storage of CO_2 from power plants, oil refineries and heavy chemical industries [4]. There are some difficulties in this technology like requirement of shared vision, international collaboration among governments. The post combustion type conventional technology uses amine absorber and the cryogenic cooler to separate CO_2 from the flue gas [5] but the amine scrubber needs more energy requirement, which makes the method less energy-efficient. The dimensions of various GHGs are relatively small, which makes the separation procedure difficult. But the difference in electronic property of the gases and that of the adsorbents are the key factor for selective separation. CO_2 has higher quadruple moment over N_2 which makes the selective adsorption of CO_2 over N_2 [6]. The proper tuning of molecular level is very essential for the CO_2 capture because only this type of strategy can take the advantage of chemical reactivity differences of the gas molecules.

Solid porous adsorbents are very demanding in the context of energy and environmental research. Huge numbers of microporous and mesoporous inorganic or organic-inorganic hybrid materials have been reported for CO_2 storage. From the inorganic platform, functionalized materials such as polyethylene amine tethered periodic MCM-41, polyaziridine coated silica, iridium complex etc. shows excellent efficiency for CO_2 uptake [7], but lack of stability is the key issue for this class of materials. Metal organic frameworks (MOFs) are known as the predominant member for the CO_2 storage material [8] because of their two or three dimensional porous framework with large accessible surface areas and huge pore volume. On the other hand, a wide range of crosslinked porous organic polymers bearing active functional groups has been developed in recent times and they have huge potential in selective gas adsorption [9].

Recently Yaghi et al. have carried out the interior modification of IRMOF-74-III by amino group to produce IRMOF-74-III-CH_2NH_2, which act as an excellent hybrid adsorbent for selective adsorption of CO_2 under humid conditions [10]. Many triazole based MOF structures modified with amine functionality [11], zeolitic imidazolate frameworks [12], acrylamide anchored MOFs [13] etc. are reported for efficient scaffold for reversible CO_2 storage. High surface area, presence of N-donor sites and tunable pore size are responsible for reversible CO_2 storage and higher CO_2/N_2 selectivity. However, major drawback of the MOF material is the difficulty in their synthesis in the large scale to meet the industry demand. Pure microporous carbon based materials such as covalent organic framework (COFs) [14], porous organic polymers [15], hypercrosslinked polymers (HCPs) [16], resins [17] N-doped microporous carbon [18], POFs [19] etc. have shown tremendous potential in the CO_2 storage applications. Further, it is very challenging to control the organic building block in the porous structure to enhance the adsorption capacity and the selectivity of CO_2. Chen et al. have reported the microporous

polycarbazole [20] of very high surface area together with very good CO_2 storage capacity. Mu et al. have reported carbazole based material MFCMP-1 [21] through an easy one step polymerization process, which showed a remarkable CO_2 storage capacity. Related porous polymers like PAF [22], FCDTPA [23] etc. have also the remarkable CO_2 uptake efficiency. Covalent triazine functionalized conjugated framework is also another important class of materials for selective CO_2 adsorption [24]. Zhou et al. have highlighted a highly porous host PPN and subsequent introduction of polar group in order to enhance the CO_2 uptake capacity [25]. These materials are advantageous over MOFs, silica, alumina based material because they have very high physicochemical stability with permanent porosity, highly scalable and can be synthesized without using any expensive catalyst or sophisticated techniques etc. Porous adsorbent having high CO_2 storage capacity and high CO_2/N_2 selectivity are very demanding in the context of separation of flue gas mixture and thus boosting the isoteric heat of adsorption by increasing the CO_2-philicity of porous solid adsorbent is very challenging.

Herein, we report a new strategy for maximum incorporation of N-containing polar functionality by using triazine containing trimodal crosslinker in polycarbazolic (Scheme 1, A_1+B_1, SB-TRZ-CRZ) and poly triphenylamine (Scheme 1, A_1+B_2, SB-TRZ-TPA) networks. We have modified the typical methodology of Lewis acid catalyzed Friedel-Craft reaction and these materials showed large reversible CO_2 uptake. To the best of our knowledge these materials displayed unprecedented CO_2/N_2 selectivity among all HCPs. This can be attributed to high BET surface area and the presence of high density triazine moieties (N-rich centers) in the framework. These porous polymers are thoroughly characterized and their selective CO_2 capture application has been explored.

2. Experimental Section

2.1. Chemicals

4-(Bromomethyl)benzonitrile, carbazole, triphenylamine were purchased from Sigma Aldrich, India. Triflic acid was purchased from spectrochem, India. Anhydrous $AlCl_3$ and all other remaining organic solvents were taken from E-Merck, India and used without further purification. 2,4,6-Tris[4-(bromomethyl)phenyl]-1,3,5-triazine was synthesized by the previously reported procedure (ESI S1).

2.2. Material Characterization

^{1}H and ^{13}C NMR studies were carried out using Bruker DPX-300 NMR spectrometer. Carbon, hydrogen and nitrogen contents of SB-TRZ-CRZ and SB-TRZ-TPA were evaluated by Perkin Elmer 2400 Series II CHN analyzer. X-Ray powder diffraction patterns of the samples were obtained with a Bruker AXS D_8 Advanced SWAX diffractometer using Cu Kα (= 0.15406 nm) radiation. Volumetric nitrogen adsorption/desorption experiments, Brunauer–Emmett–Teller (BET) specific surface area, pore volume and micropore analysis etc were carried out at 77 K using Autosorb 1 (Quantachrome, USA). CO_2 adsorption/desorption experiments at of the materials was recorded by using a Bel Japan Inc. Belsorp-HP at 273 K and room temperature. Prior to adsorption measurement the samples were degassed in vacuum at 140 ^{0}C for about 5 h. NLDFT pore-size distributions were obtained from the adsorption/desorption isotherms by using the carbon/slit-cylindrical pore model. The ^{13}C cross-polarization magic angle spinning (CP-MAS) NMR spectrum was obtained on a 500 MHz Bruker advance II spectrometer at a mass frequency of 8 kHz. Thermogravimetry analysis (TGA) and differential thermal analyses (DTA) of the samples were carried out in a TGA Instruments thermal analyzer TA-SDT Q-600. A Hitachi S-5200 field-emission scanning electron microscope was used for the determination of the morphology of the particles. Transmission electron microscopy (TEM) images were obtained

using a JEOL JEM 2010 transmission electron microscope operating at 100 kV. The samples were prepared by dropping a colloidal solution onto the carbon-coated copper grids followed by drying under high vacuum. The ^{1}H and ^{13}C NMR spectra were obtained from Bruker AVANCE III-400 MHz spectrometer. ^{1}H NMR spectra were collected at 400 MHz with chemical shift referenced to the residual peak in $CDCl_3$ (δ: H 7.26ppm. Multiplicities are written as s (singlet), d (doublet), t (triplet), m (multiplet) and br (broad). The Clausius–Clapeyron equation was used to calculate the enthalpies of adsorption for CO_2 for SB-TRZ-CRZ and SB-TRZ-TPA. In each case, the data were obtained using the equation: $(\ln P)_n = -(Q_{st}/R)(1/T) + C$, where P indicates pressure, n is the adsorbed amount, T for temperature, R is the universal gas constant and C is a constant. The isosteric heat of adsorption Q_{st} was calculated from the slope of plots of $(\ln P)_n$ as a function of 1/T.

2.3. Synthesis of SB-TRZ-CRZ

Triazine containing microporous polymer was synthesized by using the Friedel-Crafts alkylation reaction between 2,4,6-tris[4-(bromomethyl)phenyl]-1,3,5-triazine (A_1) and carbazole (B_1). In a typical synthesis 2,4,6-tris[4-(bromomethyl)phenyl]-1,3,5-triazine (1.17g, 2 mmol) and carbazole (0.25g, 1.5 mmol) were mixed in anhydrous DCM. Then 0.8g of anhydrous $AlCl_3$ was added to that solution and the mixture turned into red. It was then stirred at room temperature for 2 h under N_2 atmosphere. Then the temperature was raised to 80 ^{0}C and refluxed for 18h. The precipitate was then filtered and washed by plenty of methanol using a Soxhlet apparatus. The material was washed by acetone, THF, hexane successively and then pale greenish colored material (SB-TRZ-CRZ) obtained, which was dried under high vacuum for overnight. The yield of the reaction was 89% (1.26 g).

2.4. Synthesis of SB-TRZ- TPA

This material was synthesized by the same procedure described above using 2,4,6-tris[4-(bromomethyl)phenyl]-1,3,5-triazine (1.17g, 2 mmol) (A_1) and triphenylamine (0.49 g, 2 mmol) (B_2). The yield of the reaction is ~92 % (1.5 g).

3. Result and Discussion

C_3 symmetric tri-podal building block is very attractive for synthesizing polymeric porous frameworks. Here a triazine containing tripodal cross-linker has been used to knit the N-containing aromatics in the polymer network. Lewis acid catalyzed Friedel-Craft alkylation reaction, a well established protocol has been employed to form hypercrosslinked microporous structure with permanent and stable porosity. Several attempts had been made to introduce the polar functionality in the network in order to achieve higher CO_2 storage capacity. Here this cross-linker has a higher reactivity than other conventional ones due to triazine's electron withdrawing effect. This tripodal electrophile acts a doping agent of triazine in the polymeric network. Anhydrous aluminium chloride is used as a catalyst to make those materials. We had picked anhydrous $FeCl_3$ for this alkylation reaction but it led to the generation of undesired iron nanoparticle entrapped in the framework. $AlCl_3$ catalyzed reaction between 2,4,6-tris(4-(bromomethyl)phenyl)-1,3,5-triazine (TRZ) and carbazole (CRZ) has produced the greenish yellow thick mass and subsequent filtration and several washing by methanol, acetone and THF gave the greenish yellow light weighted powder of SB-TRZ-CRZ and the reaction between TRZ and triphenylamine (TPA) gave the brown material SB-TRZ-TPA after filtration and repeated washing with different organic solvent. These materials are not soluble in any common organic solvents.

In order to obtain the bonding and structural information of SB-TRZ-CRZ and SB-TRZ-TPA at the molecular level, FT-IR and ^{13}C CP/MAS NMR spectroscopic data had been recorded. The strong absorption at 1513 cm^{-1} for SB-TRZ-CRZ and the peak at 1509 cm^{-1} for SB-TRZ-TPA indicates the presence of triazine unit in the porous framework [26]. The peak at 1361 cm^{-1} (SB-TRZ-CRZ) and 1360 cm^{-1} (SB-TRZ-TPA) are for in plane stretching vibration of triazine ring. Peaks at 805 (SB-TRZ-CRZ) and 815 cm^{-1} (SB-TRZ-TPA) could be attributed to the breathing vibration for the triazine ring. There is no prominent peak in the range of 500-700 cm^{-1}, which confirmed that complete condensation of the monomers has been achieved (Figure 1). ^{13}C cross polarization magic angle spinning (CP-MAS) NMR had been taken to estimate the structural integrity of two type of porous framework. SB-TRZ-CRZ and SB-TRZ-TPA showed the peak at ~ 168 ppm, a characteristic peak of sp^2 carbon of triazine unit [27]. The peaks near 148 and 109 ppm for SB-TRZ-CRZ are the indicative for the two carbazolic carbon, respectively for [f] and [g]. The various carbons come from the triazinyl phenyl unit and carbazolic unit, are responsible for the most intense peak at 129 ppm which is shown in the Figure 2 (down). SB-TRZ-TPA showed an intense peak at 130 ppm with a small hump at 136 ppm, respectively and these are assigned to the phenyl ring of triphenylamine and triazine substituted phenyl ring as shown in the Figure 2 (up). The peak corresponding to benzylic carbon for SB-TRZ-CRZ is at ~ 40 ppm and for SB-TRZ-TPA at ~ 38 ppm [28], can be attributed to different electronic effect of carbazole and triphenylamine upon C_3 symmetric tris-crosslinker. Both materials are purely amorphous in nature and did not show any peak in wide angle X-ray powder diffraction. The thermal stability of SB-TRZ-CRZ and SB-TRZ-TPA has been estimated by thermogravimetric analysis (TGA). It revealed that SB-TRZ-TPA is thermally more stable than SB-TRZ-CRZ. SB-TRZ-TPA is quite stable upto 400 ^0C and whereas SB-TRZ-CRZ undergoes roughly 5% weight

loss at nearly 150 ^{0}C due to loss of some solvent molecule or water entrapped in the network followed by structural cleavage above 300 ^{0}C. Thus, SB-TRZ-CRZ is stable upto 300 ^{0}C (ESI S4).

3.1. Porosity Measurement

The porous nature of the hypercrosslinked structure is revealed from the sorption analysis using N_2 gas as an adsorbate molecule. The N_2 adsorption/desorption isotherms are measured at 77 K is shown in the Figure 3 SB-TRZ-CRZ showed a typical type I isotherm, which suggested the pure microporous nature [29] of this carbazole based framework according to the IUPAC classification. SB-TRZ-TPA also displayed a type I nature in its adsorption/desorption isotherms. The Brunauer–Emmett–Teller (BET) specific surface area of SB-TRZ-CRZ is 642 m^2g^{-1} (ESI S5) and that of SB-TRZ-TPA is 310 m^2g^{-1} (Figure 3a).The pore size distribution of the two triazine based materials are calculated using the non-local density functional theory (NLDFT) theory and carbon slit pore model. The predominant pore sizes as estimated from the respective pore size distribution plots for these materials are 1.7 nm for SB-TRZ-CRZ and 1.5 nm for SB-TRZ-TPA, which suggested that both materials possess extremely large micropores/supermicropores (Figure 3b). The pore volumes of SB-TRZ-CRZ and SB-TRZ-TPA are 0.2888 and 0.1469 ccg^{-1}, respectively (Table 1).

3.2. Microstructural Analysis

The particle morphology of the two networks is determined with the help of field emission scanning electron microscopic (FE-SEM) and high resolution transmission electron microscopic (HRTEM) analyses. FE-SEM images suggested particle morphology of microporous triazine knitted carbazole networks of SB-TRZ-CRZ is composed of submicron spheres of average diameter 350-450 nm (Figures 4a,b) at different magnification. SB-TRZ-TPA

is composed of small agglomerated inter grown particles with average diameter 450-600 nm (Figures 4c,d). High-resolution transmission electron microscopic (TEM) images of both these porous polymers indicated that they are composed of very tiny particles with interparticle void spaces (Figures 4e,f).

3.3. Reversible CO_2 Capture

Enhancing CO_2-philicity of the porous network is a big challenge to increase the CO_2 uptake capacity. Recently it is reported that carbon based porous adsorbent should be functionalized in such way that the network will able to create a pronounced magnetic field at the surface that CO_2 can interact extensively with the porous host via its quadruple interaction [30]. Generally the presence of nitrogen atom in the carbon scaffold increases the affinity of the network towards CO_2 because of facilitated dipole-quadrapole interaction [31]. Several microporous polycarbazole, poly triphenylamine are known for good CO_2 storage material [32]. Here we have investigated the doping effect of triazine into porous N-containing microporous polymer and the change of the CO_2 storage efficiency using a triazine containing tripodal crosslinker. The loading of triazine moiety in the polycarbazole and polytriphenyl network has been optimized by using various molar ratios of the individual monomers. Faul et al. have synthesized several poly triphenylamine via Buchwald–Hartwig coupling having the CO_2 uptake capacity 6.5 wt% [33]. Dai et al. have synthesized various modified polycarbazoles such as (P-PCz) [34], TSP-1, TSP-2 etc in order to boost the CO_2 uptake capacity and the uptake capacities are respectively 5.57 mmol g^{-1}, 18 wt%. Han et al. have synthesized the polycarbazole [35] (CPOP-16-19) having CO_2 uptake capacity of 16.7 wt% upto 1 bar 273 K.

Here we have incorporated triazine moiety in the N-containing porous polymeric backbones, which is very desirable for post combustion CO_2 capture application [36]. SB-TRZ-

CRZ has shown the 25.5 wt% CO_2 uptake upto 1 bar at 273 K and 44.5 wt % upto 3 bar at 273 K (Figure 5a). It also has shown remarkable CO_2 uptake upto 3 bar at room temperature [37] (13.9 wt%). SB-TRZ-TPA has shown 29.8 wt% CO_2 uptake upto 3 bar at 273 K and nearly 16 wt % (upto 1 bar) at 273 K (Figure 5c). SB-TRZ-TPA exhibits the CO_2 uptake of 11 wt% at room temperature (303 K) (Table 1). So it is clear that the method of doping of triazine into polycarbazole and poly triphenylamine in our work significantly effective toward CO_2 storage application. The CO_2 philicity of the polymeric network has tremendously increased from previously reported modified polycarbazole and polytriphenylamine. CO_2 uptakes of these two materials are also very comparable with previously best reported COFs [38,39], MOFs [40,41], N-doped microporous carbons [42,43], hypercrosslinked porous polymers [44-46], etc. The high density of basic nitrogen sites of triazine present in the polymer network which interact with ewis acidic CO_2 molecules via dipole quadrapole interaction, are responsible for huge CO_2 uptake [47]. Further, large CO_2 uptake capacity for these materials can be attributed to the high degree of crosslinking between the monomers used to construct the hypercrosslinked structure which leads to high concentration of triazine and N-containing arenes in the network. The degree of elastic expansion of porous structure (swelling) creates the difference between the deformed pore volume and true pore volume which manifests in the N_2 adsorption/desorption isotherm at 77 K.

3.4. CO_2/N_2 selectivity

In-spite-of moderate surface area of SB-TRZ-CRZ and SB-TRZ-TPA they displayed huge CO_2 uptake and thus it is necessary to investigate the preferential uptake of CO_2 over N_2 to understand the efficacy of gas separation application. The selectivity of the gas uptake towards CO_2 over N_2 is measured by volumetric measurement of pure gas physisorption isotherm at 273

K. The microporous polymer having larger surface area will definitely have the higher CO_2 uptake capacity but it is very challenging to tune the organic building blocks of the polymeric network in such a way that CO_2 uptake capability will be much higher considering its relatively low surface area and thus those materials will come with a excellent selectivity of CO_2/N_2. As seen in Figures 5a and 5c, the CO_2 adsorption curves are following the linear trend with increasing the pressure whereas N_2 exhibited no significant uptake. SB-TRZ-CRZ has shown 5.7 mmol/g CO_2 uptake upto 1 bar at 273 K and ~10 mmol/g upto 3 bar. On the other hand SB-TRZ-TPA has shown 3.6 mmol/g CO_2 uptake upto 1 bar and 6.7 mmol/g upto 3 bar at 273 K. The CO_2/N_2 selectivity has been calculated by taking the ratio of two initial slopes of the isotherms of CO_2 and N_2. The calculated CO_2/N_2 selectivity of SB-TRZ-CRZ and SB-TRZ-TPA are 377:1 (Figure 5b) and 97:1 (Figure 5d), , respectively at 273 K. As far as we know these selectivity values are precisely comparable with those of recently reported hypercrosslinked polymers (Th-1, Py-1, Fu-1 [48], anyline-benzene co-polymer network [49], hydroxyl containing MOPs [50]), COFs(ILCOF-1[51], 3D-Py-COF [52]), MOFs [53,54] and porous carbons [55]. By measuring the CO_2 adsorption isotherm at different temperature and applying Clausius-Claperyron equation, we have calculated isoelectric heat of adsorption, and corresponding values are in the range of 32-38 kJ/ mol for SB-TRZ-CRZ (Figure 6a) and 34-35 kJ/ mol for SB-TRZ-TPA (Figure 6b) which is higher than triazine based poly-benzimidazole (TBILP-1) [56] and comparable to ultramicroporous poly-benzimidazole (BILP-101) [57], recently reported hypercrosslinked polymer (Figure 7).

4. Conclusion

Triazine functionalized two new microporous polymers SB-TRZ-CRZ and SB-TRZ-TPA have been synthesized by one step, easy Lewis acid catalyzed Friedel-Crafts alkylation reaction

using a triazine containing tripodal crosslinker, which knitted carbazole and triphenylamine molecules, and resulted efficient incorporation of triazine in polycarbazole and poly-triphenylamine networks. These materials have high BET surface areas 642 m^2g^{-1} (SB-TRZ-CRZ) and 310 m^2g^{-1} (SB-TRZ-TPA). The CO_2 uptake capacity of SB-TRZ-CRZ is 25.5 wt% upto 1 bar at 273 K and SB-TRZ-TPA is 16 wt % under identical conditions. Selective gas adsorption analysis revealed that SB-TRZ-CRZ has a CO_2/N_2 selectivity of 377 and SB-TRZ-TPA has the selectivity of 97. Synthesis of these novel hypercrosslinked microporous materials and their large carbon dioxide uptakes reported herein may contribute significantly in developing an efficient adsorbent for environmental remediation.

Acknowledgments

SB and PB wish to thank CSIR, New Delhi and SKD wish to thank UGC, New Delhi for their respective Senior and Junior Research Fellowships. AB and TS wish to thank DST, New Delhi and British Council, UK for providing research grants through DST-UKIERI project.

Notes and References

[1] N. Y. Du, H. B. Park, M. M. Dal-Cin, M. D. Guiver, Energy Environ. Sci. 5 (2012) 7306-7322.

[2] M. Meinshausen, N. Meinshausen, W. Hare, S. C. B. Raper, K. Frieler, R. Knutti, D. J. Frame, M. R. Allen, Nature 458 **(**2009) 1158-1162.

[3] D. Aaron , C. Tsouris, Separation Sci. Technol. 40 **(**2005) 321-348.

[4] M. E. Boot-Handford, J. C. Abanades, E. J. Anthony, M. J. Blunt, S. Brandani, N. Mac Dowell, J. R. Fernandez, M. C. Ferrari, R. Gross, J. P. Hallett, R. S. Haszeldine, P. Heptonstall, A. Lyngfelt, Z. Makuch, E. Mangano, R. T. J. Porter, M. Pourkashanian, G. T. Rochelle, N. Shah, J. G. Yao, P. S. Fennell, Energy Environ. Sci. **7** (2014) 130-189.

[5] M. Mofarahi, Y. Khojasteh, H. Khaledi, A. Farahnak, Energy 33 (2008) 1311-1319.

[6] Q. Q. Dang, Y. F. Zhan, X. M. Wang, X. M. Zhang, ACS Appl. Mater. Interfaces **7** (2015) 28452-28458.

[7] N. D. McNamara, J. C. Hicks, ChemSusChem **7** (2014) 1114-1124.

[8] A. R. Millward, O. M. Yaghi, J. Am. Chem. Soc. 127 (2005) 17998-17999.

[9] D. M. D'Alessandro, B. Smit, J. R. Long, Angew. Chem. Int. Ed. 49 (2010) 6058-6082.

[10] A. M. Fracaroli, H. Furukawa, M. Suzuki, M. Dodd, S. Okajima, F. Gándara, J. A. Reimer, O. M. Yaghi, J. Am. Chem. Soc. 136 (2014) 8863-8866.

[11] J. -J. Hou, X. Xu, N. Jiang, Y. –Q. Wu, X. –M. Zhang, J. Solid State Chem. 223 (2015) 73-78.

[12] R. Banerjee, A. Phan, B. Wang, C. Knobler, H. Furukawa, M. Ókeeffe, O. M. Yaghi, Science 319 (2008) 939-943.

[13] B. Zheng, J. Bai, J. Duan, L. Wojtas, M. J. Zaworotko, J. Am. Chem. Soc. 133 (2011) 748-751.

[14] R. Gomes, P. Bhanja and A. Bhaumik, Chem. Commun. 51 (2015) 10050-10053.

[15] S. Ren , M. J. Bojdys , R. Dawson , A. Laybourn , Y. Z. Khimyak , D. J. Adams, A. I. Cooper, Adv. Mater. 24 (2012) 2357-2361.

[16] S. Bhunia, B. Banerjee, A. Bhaumik, Chem. Commun. 51 (2015) 5020-5023.

[17] A. P. Katsoulidis, M. G. Kanatzidis, Chem. Mater. 23 (2011) 1818-1824.

[18] M. Nandi, K. Okada, A. Dutta, A. Bhaumik, J. Maruyama, D. Derks, H. Uyama, Chem. Commun. 48 (2012) 10283-10285.

[19] A. P. Katsoulidis, S. M. Dyar, R. Carmieli, C. D. Malliakas, M. R. Wasielewski, M. G. Kanatzidis, J. Mater. Chem. A 1 (2013) 10465-10473.

[20] Q. Chen, M. Luo, P. Hammershøj, D. Zhou, Y. Han, B. W. Laursen, C. –G. Yan, B. –H. Han, J. Am. Chem. Soc. 134 (2012) 6084-6087.

[21] Y. Zhang, S. A, Y. Zou, X. Luo, Z. Li, H. Xia, X. Liu, Y. Mu, J. Mater. Chem. A 2 (2014) 13422-13430.

[22] T. Ben, C. Pei, D. Zhang, J. Xu, F. Deng, X. Jing, S. Qiu, Energy Environ. Sci. 4 (2011) 3991-3999.

[23] X. Yang, M. Yu, Y. Zhao, C. Zhang, X. Wang, J. –X. Jiang, J. Mater. Chem. A 2 (2014)

15139-15145.

[24] X. Zhu, C. Tian, S. M. Mahurin, S. –H. Chai, C. Wang, S. Brown, G. M. Veith, H. Luo, H. Liu, S. Dai, J. Am. Chem. Soc. 134 (2012) 10478-10484.

[25] W. Lu, D. Yuan, J. Sculley, D. Zhao, R. Krishna, H. –C. Zhou, J. Am. Chem. Soc. 133 (2011) 18126-18129.

[26] W. Zhang, C. Li, Y. –P. Yuan, L. –G. Qiu, A. –J. Xie, Y. –H. Shen, J. –F. Zhu, J. Mater. Chem. 20 (2010) 6413-6415.

[27] B. Jürgens, E. Irran, J. Senker, P. Kroll, H. Müller, W. Schnick, J. Am. Chem. Soc. 125 (2003) 10288-10300.

[28] Y. Luo, S. Zhang, Y. Ma, W. Wang, B. Tan, Polym. Chem. 4 (2013) 1126-1131.

[29] W. Lu, J. P. Sculley, D. Yuan, R. Krishna, Z. Wei, H. –C. Zhou, Angew. Chem. Int. Ed. 51(2012) 7480-7484.

[30] P. Raveendran, Y. Ikushima, S. L. Wallen, Acc. Chem. Res. 38 (2005) 478-485.

[31] M. Khajehpour, J. F. Kauffman, J. Phys. Chem. A 104 (2000) 9512-9517.

[32] F. Jiang, J. Sun, R. Yang, S. Qiao, Z. An, J. Huang, H. Mao, G. Chen, Y. Ren, New J. Chem. 2016 DOI: 10.1039/C5NJ03215F.

[33] Y. Liao, J. Weber, C. F. J. Faul, Chem. Commun. 50 (2014) 8002-8005.

[34] T. Jin, Y. Xiong, X. Zhu, Z. Tian, D. –J. Tao, J. Hu, D. Jiang, H. Wang, H. Liu, S. Dai, Chem. Commun. 52 (2016) 4454-4457.

[35] L. Pan, Q. Chen, J. –H. Zhu, J. –G. Yu, Y. –J. He, B. –H. Han, Polym. Chem. 6 (2015)

2478-2487.

[36] B. Li, Z. Zhang, Y. Li, K. Yao, Y. Zhu, Z. Deng, F. Yang, X. Zhou, G. Li, H. Wu, N. Nijem, Y. J. Chabal, Z. Lai, Y. Han, Z. Shi, S. Feng and J. Li, Angew. Chem. Int. Ed. 51 (2012) 1412-1415.

[37] A. R. Millward, O. M. Yaghi, J. Am. Chem. Soc. 127 (2005) 17998-17999.

[38] P. J. Waller, F. Gándara, O. M. Yaghi, Acc. Chem. Res. 48 (2015) 3053-3063.

[39] Y. Zeng, R. Zou, Y. Zhao, Adv. Mater. 2016, DOI: 10.1002/adma.201505004.

[40] D. Britt, H. Furukawa, B. Wang, T. G. Glover, O. M. Yaghi, Proc. Natl. Acad. Sci. USA 106 (2009) 20637-20640.

[41] A. Aijaz, N. Fujiwara, Q. Xu, J. Am. Chem. Soc. 136 (2014) 6790-6793.

[42] M. Sevilla, P. V. Vigón, A. B. Fuertes, Adv. Funct. Mater. (2011) 21 2781-2787.

[43] W. Xing, C. Liu, Z. Zhou, L. Zhang, J. Zhou, S. Zhuo, Z. Yan, H. Gao, G. Wang, S. Z. Qiao, Energy Environ. Sci. 5 (2012) 7323-7327.

[44] R. T. Woodward, L. A. Stevens, R. Dawson, M. Vijayaraghavan, T. Hasell, I. P. Silverwood, A. V. Ewing, T. Ratvijitvech, J. D. Exley, S. Y. Chong, F. Blanc, D. J. Adams, S. G. Kazarian, C. E. Snape, T. C. Drage, A. I. Cooper, J. Am. Chem. Soc. 136 (2014) 9028-9035.

[45] M. G. Rabbani, T. E. Reich, R. M. Kassab, K. T. Jackson, H. M. El-Kaderi, Chem. Commun. 48 (2012) 1141-1143.

[46] X. Jing, D. Zou, P. Cui, H. Ren, G. Zhu, J. Mater. Chem. A 1 (2013) 13926-13931.

[47] R. Vaidhyanathan, S. S. Iremonger, G. K. H. Shimizu, P. G. Boyd, S. Alavi, T. K. Woo, Science 330 (2010) 650-653.

[48] Y. Luo, B. Li, W. Wang, K. Wu, B Tan, Adv. Mater. 24 (2012) 5703-5707.

[49] R. Dawson, T. Ratvijitvech, M. Corker, A. Laybourn, Y. Z. Khimyak, A. I. Cooper, D. J. Adams, Polym. Chem. 3 (2012) 2034-2038.

[50] R. Dawson, L. A. Stevens, T. C. Drage, C. E. Snape, M. W. Smith, D. J. Adams , A. I. Cooper, J. Am. Chem. Soc.134 (2012) 10741-10744.

[51] M. G. Rabbani, A. K. Sekizkardes, Z. Kahveci, T. E. Reich, R. Ding, H. M. El-Kaderi, Chem. Eur. J. 19 (2013) 3324-3328.

[52] G. Lin, H. Ding, D. Yuan, B. Wang, C. Wang, J. Am. Chem. Soc.138 (2016) 3302-3305.

[53] D. –M. Chen, N. Xu, X. –H. Qiu, P. Cheng, Cryst. Growth Des. 15 (2015) 961-965.

[54] P. T. K. Nguyen, H. T. D. Nguyen, H. Q. Pham, J. Kim, K. E. Cordova, H. Furukawa, Inorg. Chem. 54 (2015) 10065-10072.

[55] A. Modak, A. Bhaumik, J. Solid State Chem. 232 (2015) 157-162.

[56] A. K. Sekizkardes, S. Altarawneh, Z. Kahveci, T. İslamoğlu,H. M. El-Kaderi, Macromolecules 47 (2014) 8328-8334.

[57] A. K. Sekizkardes, J. T. Culp, T. Islamoglu, A. Marti, D. Hopkinson, C. Myers, H. M. El-Kaderi, H. B. Nulwala, Chem. Commun. (2015) 51 13393-13396.

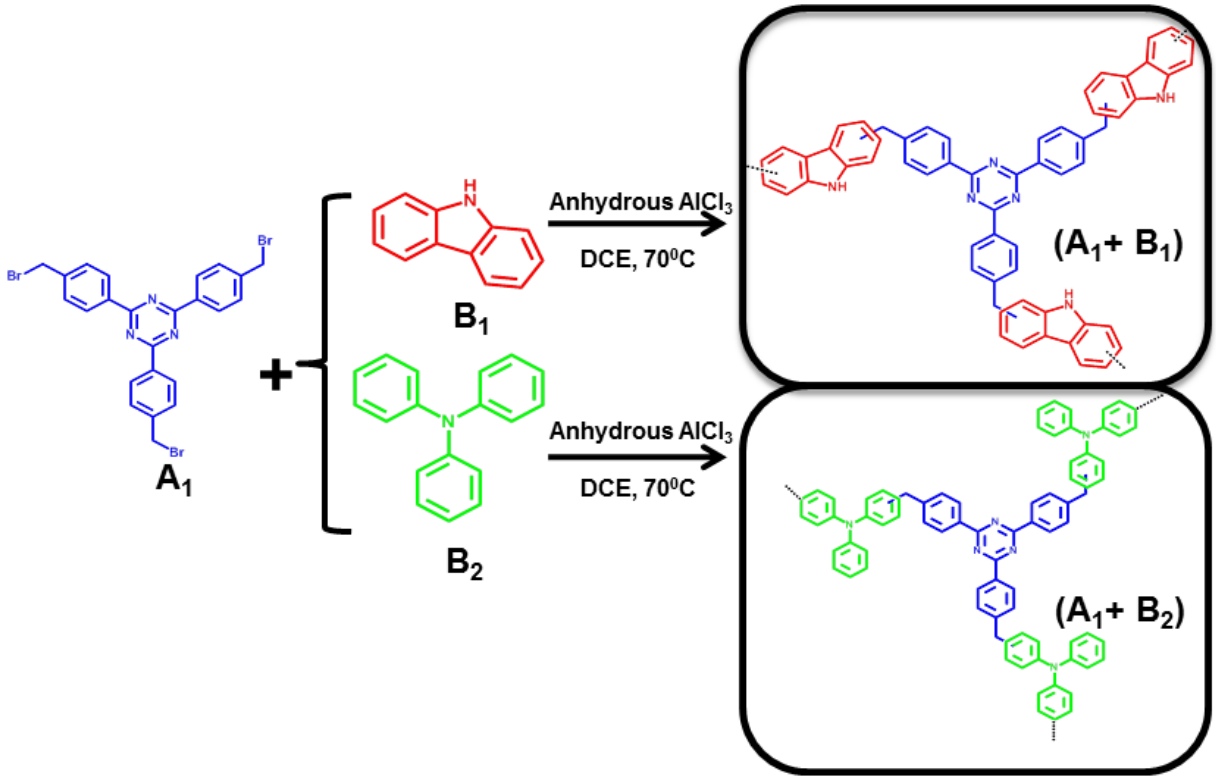

Scheme 1. Preparation of triazine doped microporous organic polymer.

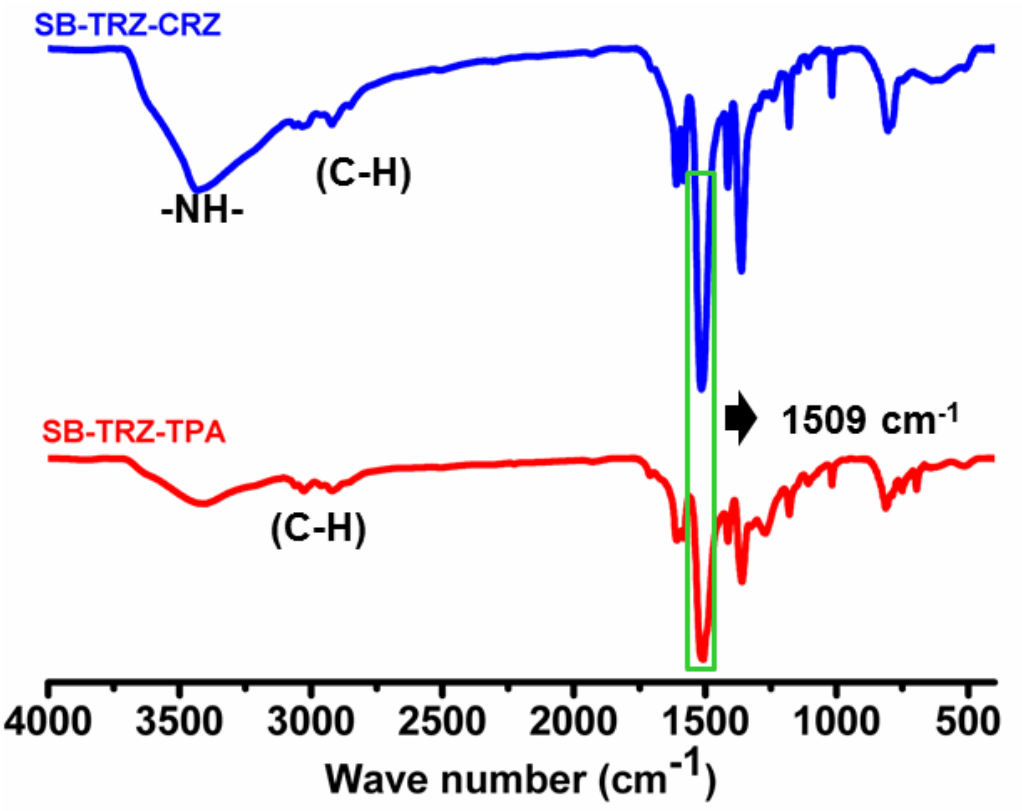

Figure 1. FT-IR spectra of SB-TRZ-CRZ and SB-TRZ-TPA

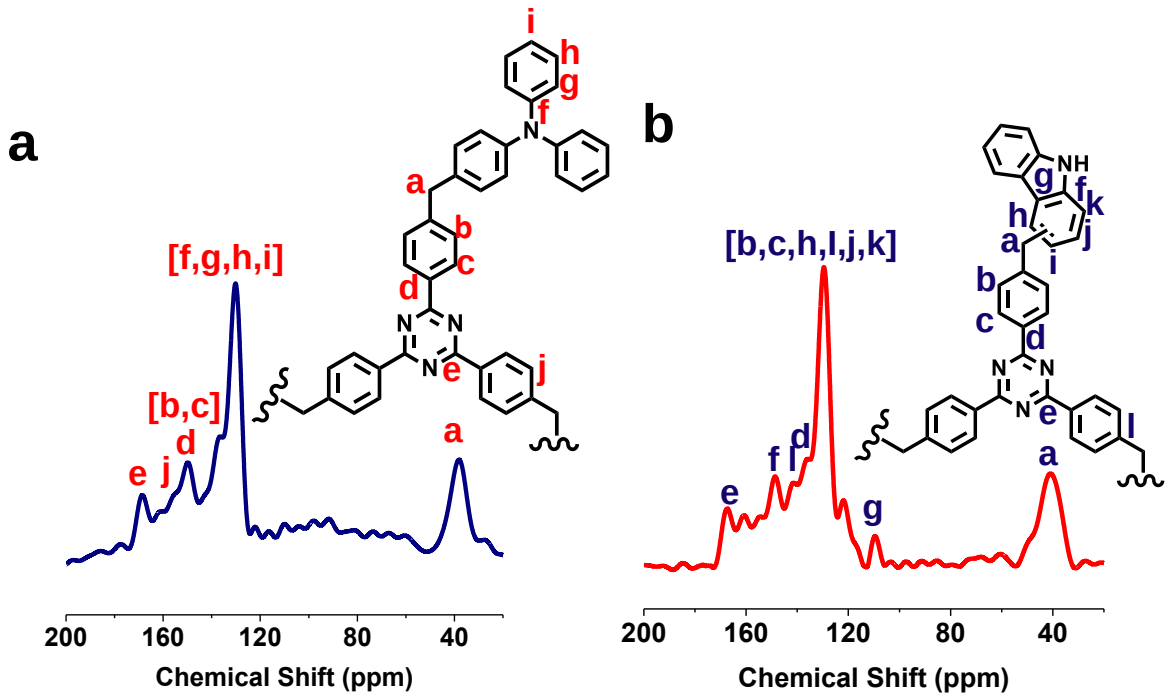

Figure 2. (a)(SB-TRZ-TPA (left, blue) (b)^{13}C CP/MAS NMR spectra of SB-TRZ-CRZ (right, red,) .

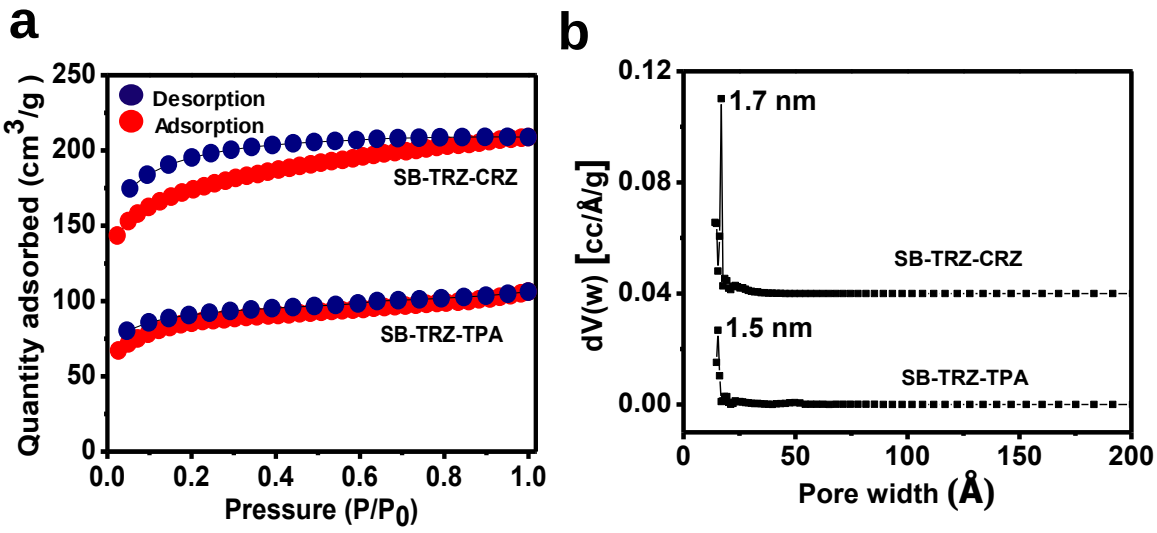

Figure 3. (a) N_2 adsorption/desorption isotherms of SB-TRZ-CRZ and SB-TRZ-TPA. Adsorption points are marked by red filled circle and desorption points by blue filled circle b) pore sized distribution of SB-TRZ-CRZ (upper) and SB-TRZ-TPA (lower) by NDLFT method.

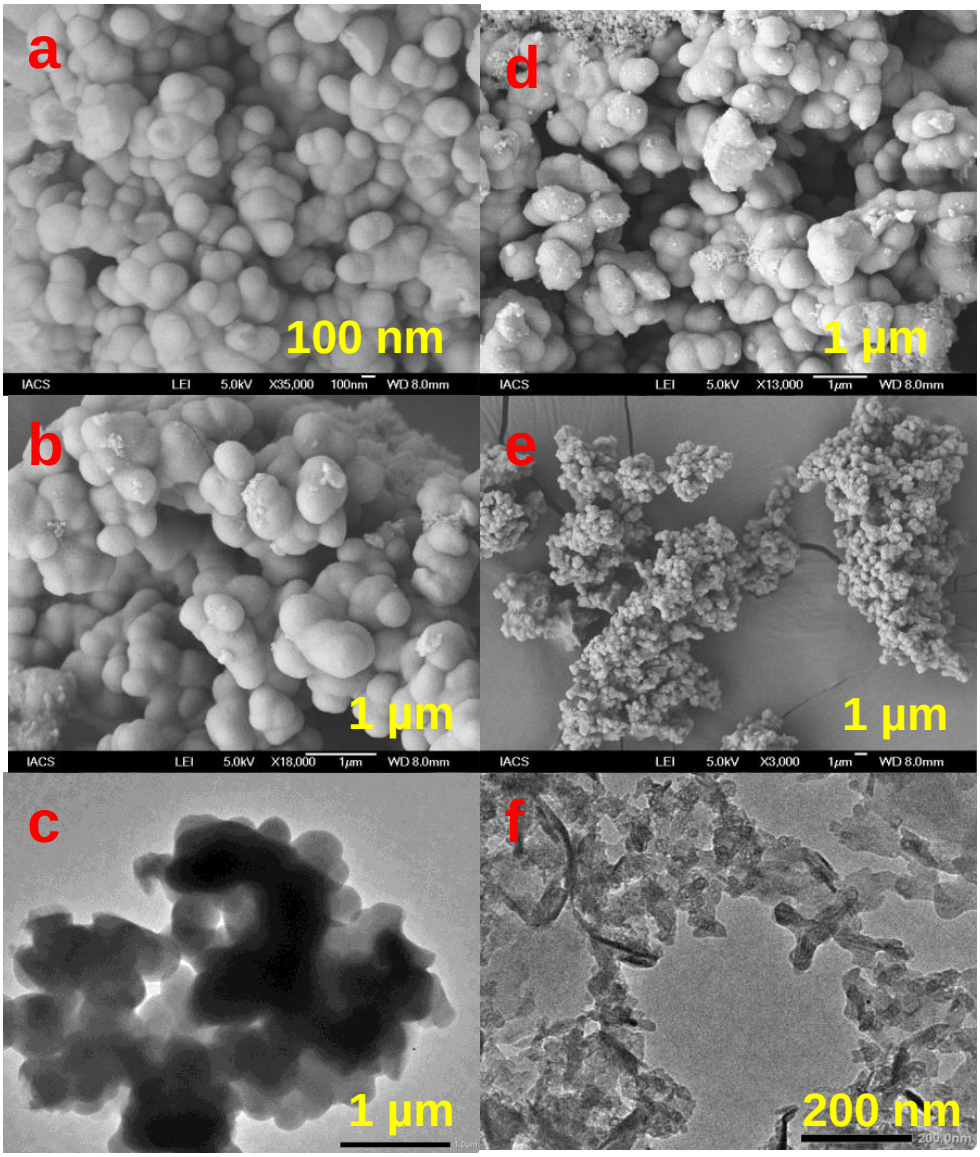

Figure 4. SEM images of SB-TRZ-CRZ at different magnification (a,b) and SB-TRZ-TPA (d,e); TEM image of SB-TRZ-CRZ (e) and SB-TRZ-TPA (f).

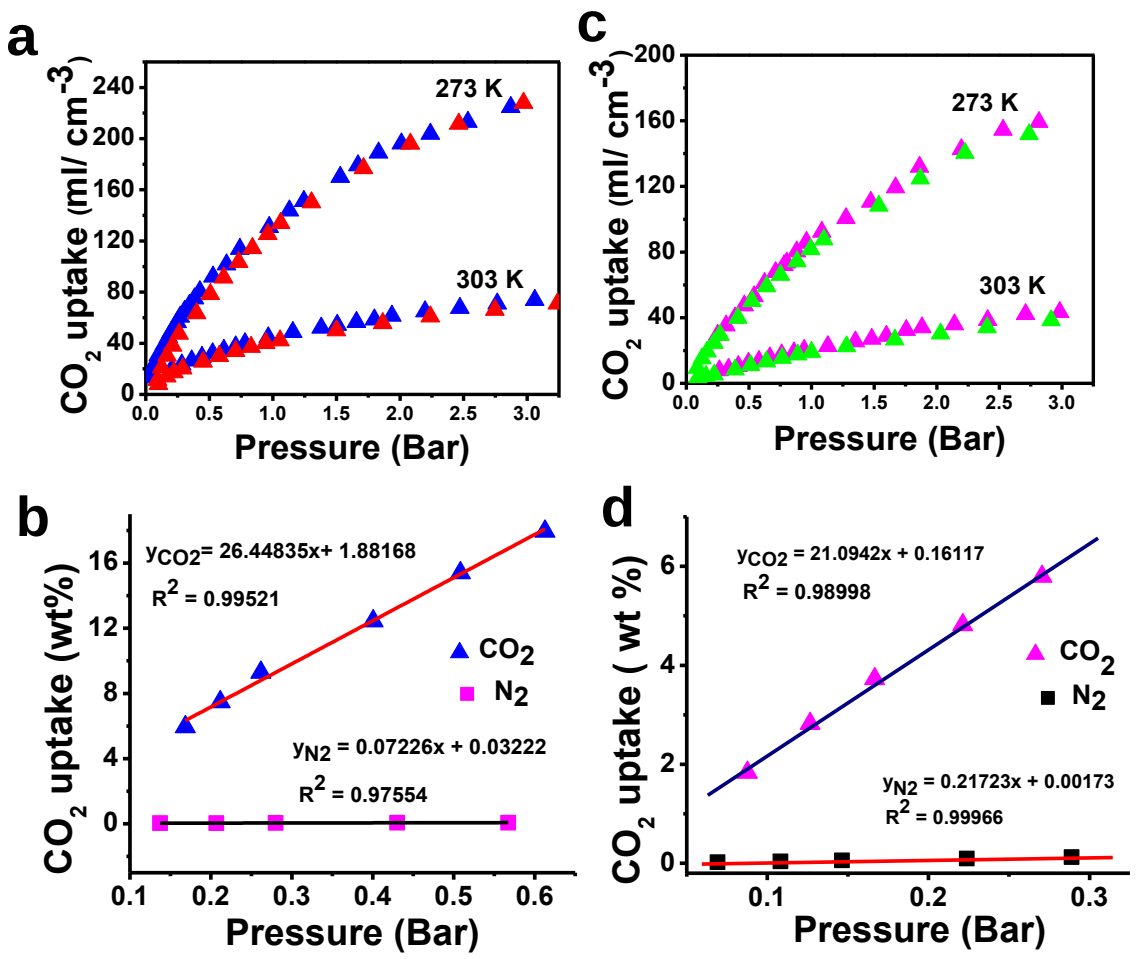

Figure 5. (a) CO_2 uptake of SB-TRZ-CRZ at 273 K and 303 K, (b) CO_2/N_2 selectivity of SB-TRZ-CRZ, (c) CO_2 uptake of SB-TRZ-TPA at 273 K and 303 K, (d) CO_2/N_2 selectivity of SB-TRZ-TPA.

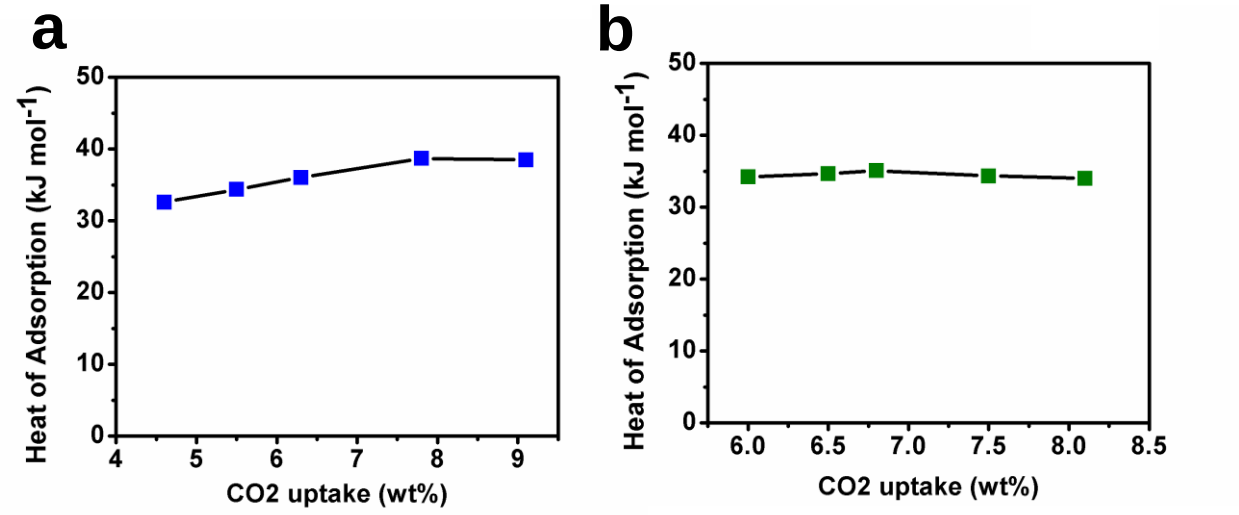

Figure 6. (a) isoelectric heat of adsorption of SB-TRZ-CRZ, (b) SB-TRZ-TPA.

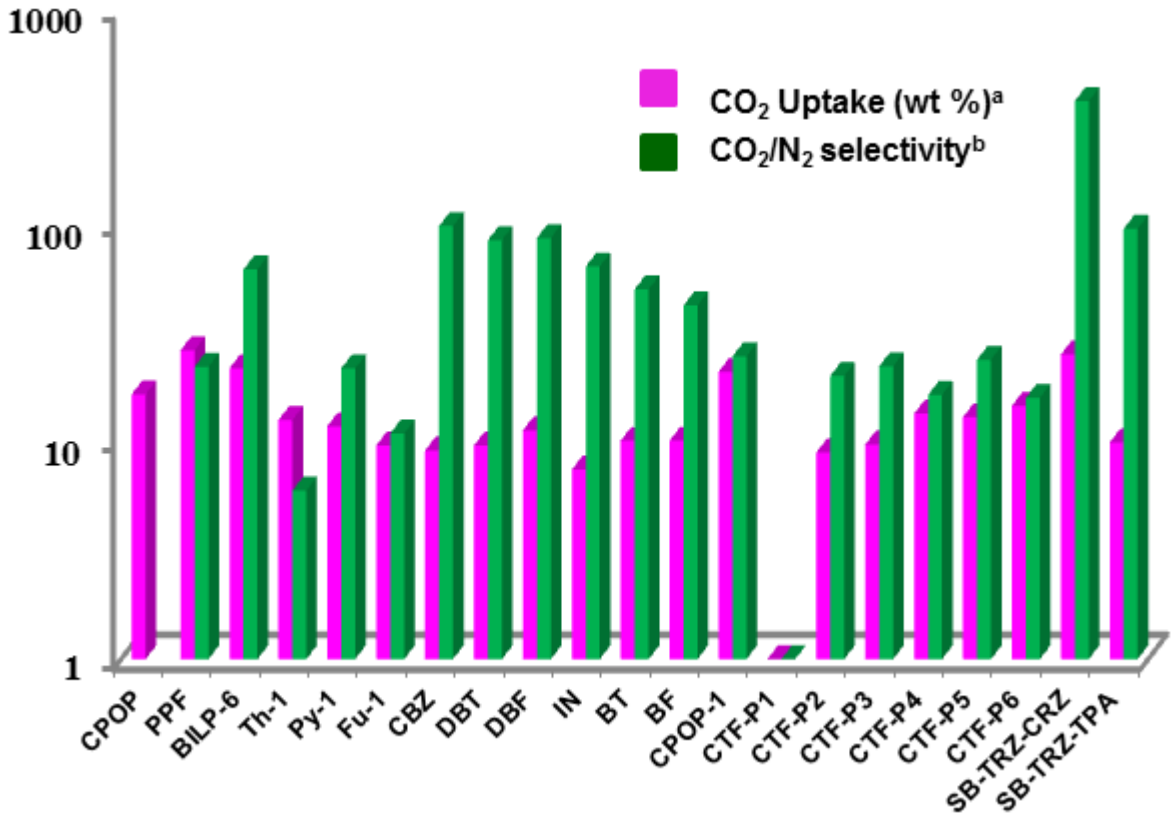

Figure 7 logarithmic presentations of CO_2 uptake and selectivity (CO_2/N_2) of SB-TRZ-CRZ and SB-TRZ-TPA with recently reported organic microporous sorbents.[48,50,51,52]

[a] CO_2 uptake has been measured at 273 K and upto 1 atm

[b] selectivity of 273 K and it has been measured by taking the slope ration of two individual isotherms (CO_2 and N_2)

Table 1 Surface area, pore property and CO_2 upake efficiency of hypercrosslinked networks.

Material	**S_{BET} (m^2/g)**	**Pore size (nm)**	**V_{total}(cc/g)**	**CO_2 Uptake(wt%)** (Upto 3 bar) 273K	298K	**CO_2/N_2 Selectivity[α]** (273K)
SB-TRZ-CRZ[a] (A1+B1)	642	1.7	0.2888	44.5	13.9	377:1
SB-TRZ-TPA[b] (A1+B2)	330	1.5	0.1469	29.8	~ 11	97:1

[a]Ratio of A1:B1= 4:3
[b] Ratio of A1:B2= 1:1
[α] Selectivity was calculated by calculating the ratio of initial slope at low pressure region.